Renewable Energy 219 (2023) 119532

Contents lists available at ScienceDirect

Renewable Energy

journal homepage: www.elsevier.com/locate/renene

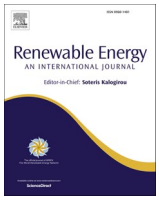

Long-term performance of pilot-scale tubular plant-microbial fuel cells in a brownfield-constructed wetland

Pim de Jager [a,b], Daniel Groen [a], David P.B.T.B. Strik [b,*]

[a] Plant-e BV, Tarthorst 823, 6708, JC, Wageningen, the Netherlands
[b] Wageningen University & Research, Environmental Technology, Bornse Weilanden 9, 6708, WG, Wageningen, the Netherlands

ARTICLE INFO

Keywords:
Plant-microbial fuel cell
Electricity
Sensor
wetland restoration
Scale-up
Tubular

ABSTRACT

The plant-microbial fuel cell (P-MFC) is a suitable stand-alone power source for low-power (mW) electronics. P-MFCs have been studied extensively under laboratory conditions. Some studies investigated P-MFCs under field conditions, usually on a small scale or for a short time. The objective of this research was to identify the performance of the tubular P-MFC over a period of years during the establishment of a constructed wetland from a brownfield that was fed with water from a ditch. The performance of tubular P-MFCs with seven different commercially available electrode materials, different depth below the surface, tube length, as well as tube diameter, was investigated by measuring voltages and temperature, as well as by performing polarization measurements. With a maximum of 13–18 mW/m^2 projected plant surface, or 1.1 mW for a 1m tube, the tubular P-MFC is expected to be a suitable power source for remote sensing equipment. The performance of the tubular P-MFC is correlated to temperature and decreases significantly at temperatures below 6 °C. Longer tubular P-MFCs produce more power, but less power per meter, where the optimum tube length seems to be around one to 2 m. Longer tubes experience higher losses due to material resistance. The tubular P-MFC design is not so sensitive to different electrode material choices, and smaller P-MFCs seem to perform relatively well. To utilize P-MFC power for sensor applications, an appropriate harvester should be designed that is able to find the maximum power point of the P-MFC while harvesting and has sufficient buffer capacity in case of temperature and seasonal variations.

1. Introduction

The plant-microbial fuel cell (P-MFC) is an emerging technology that converts organic matter into electricity using living plants and bacteria naturally present in the soil. In a P-MFC, organic matter is oxidized by electrochemically active bacteria (EAB) that use an electrode, the anode, as a terminal electron acceptor. Depending on how the systems are implemented, this organic matter can be derived from the rhizodeposits of living plants, plant waste, and soil, as well as from the influx of materials from (natural) water flows or as a combination of these sources. In addition to EAB, chemical-induced oxidation reactions can also be expected to occur in a P-MFC, especially once P-MFCs are placed into marine sediments where oxidation of sediment sulfide could play a role [1,2]. The anode is connected through an external circuit to a cathode, where oxygen from the air is reduced to water [3]. Oxygen can be reduced at the cathode abiotically as well as catalyzed by microorganisms through a biocathode [4]. P-MFC applications include "small-scale" electricity production, as well as potential methane reduction, wetland restoration and nature conservation [5–8]. The technology can be applied in natural and constructed wetlands, as well as in marine environments, or even incorporated into plants directly [9]. Wetland restoration is a recent issue that is gaining much attention [10,11] and can have multiple purposes when combined with P-MFCs. Since P-MFCs do not require external energy storage or input, the technology can be applied in remote areas without electrical infrastructure.

A potential application in which the electricity produced by P-MFCs can be used is remote sensing. As electronic sensors and microchips become cheaper and more energy efficient, small-scale wireless sensing and data collection systems are developed. These systems are often battery or photovoltaic powered and are frequently installed in remote places [12–15]. Photovoltaic cells are installed above ground, making them vulnerable for vandalism by humans or animals [16], and are dependent on light availability. Batteries can be small and hidden, but they contain rare-earth chemicals and eventually need to be replaced

* Corresponding author.
E-mail address: david.strik@wur.nl (D.P.B.T.B. Strik).

https://doi.org/10.1016/j.renene.2023.119532
Received 27 March 2023; Received in revised form 12 September 2023; Accepted 26 October 2023
Available online 27 October 2023

[17]. Although electronic sensors and microchips are becoming cheaper, the manual labor needed to change batteries is becoming proportionally more expensive and is driving the need for a stand-alone power source [18,19], [20]. P-MFCs have the potential to be this power source [21, 22].

Scale-up research and performance evaluation at prolonged periods of time under real conditions is critical for the implementation of Plant-MFC with remote sensing. Different forms of P-MFCs have been designed and described in the literature, including tubular Plant-MFC [23–25]. In many P-MFC systems, plants are planted in a reactor containing solely conductive material, which is labor intensive and may be stressful for the plant since these plants are often transplanted from natural soil into a different, conductive, substrate [26]. A tubular P-MFC system, in contrast, is buried within the subsurface of an ecosystem, which requires less labor for installation (personal communication Plant-e BV, see S2) and limited visual disturbance of the ecosystem. While many different P-MFC designs, including the tubular design, have been extensively studied, most of these studies have been carried out in the lab [27,28]. Lab studies are suitable for determining single parameters, but they do not accurately represent more dynamic, natural outdoor conditions. Some researchers have done P-MFC studies in outdoor conditions, such as Helder et al. [29] on a roof in the Netherlands and Kaku et al. [30] using a submerged anode and floating cathode in real rice paddies. However, these studies have been done on a small scale and not with tubular P-MFCs. Different studies have investigated the connection of multiple P-MFCs in series and parallel, but this strategy was not successful, causing lower power output and even total collapse due to cell reversal [31,32]. Sudirjo et al. [24] installed tubular P-MFCs in a rice paddy in Indonesia, but this was with only three 1-m(1m)-long P-MFCs. Tubular P-MFCs over 1 m in length in outdoor conditions over multiple years or seasons have not yet been investigated. Tubular P-MFCs are designed to be scalable by increasing the length of the tube to allow a higher power generation. Moreover, seasonal effects, outdoor conditions, and material variations are expected to affect the performance of tubular P-MFCs [24,29,30,33]. Although there are some studies that applied a P-MFC as a power source for remote sensing equipment, these were either under controlled (lab) environments [34,35]; [36] or for a short time [21]. There is a lack of long-term studies under real outdoor conditions. Such studies can provide confidence in the tubular P-MFC as a reliable power source, which is a sensible prerequisite for successful commercialization. Understanding the scaling effects as well as correlating environmental conditions is imminent in the design of possible solutions to provide energy for remote sensing.

The objective of this study was to investigate the performance effects of different electrode materials and configurations of scaled-up tubular P-MFCs under real outdoor wetland conditions in the Netherlands, for at least two growing seasons, those being two consecutive spring-summer periods. To make this study possible, a temporary wetland fed with water from a local ditch was constructed with ~400 m^2 surface area on a remediated brownfield, which was originally part of the large wetland system called the Loozerheide, in the Netherlands [37]. The results presented in this research are from a pilot study with 59 tubular P-MFCs, the combined length of which was more than 100 m. The following parameters were investigated in triplicate: seven different commercially available electrode materials, two different installation depths, five tube lengths, and two diameters of tubes. Dynamic performance (influenced by external parameters such as temperature and seasons) and effects of the mentioned parameters were evaluated over a total period of 26 months. Finally, the power and current production of the best performing P-MFC design was assessed, determining the potential viability of the P-MFC as a remote stand-alone power source for sensing equipment. This study therefore also contributes to the worldwide growing interest in the Internet of Things [13,14], evaluating a potential power source for small electric devices for locations and situations where there is no alternative available.

2. Materials and Methods

2.1. Experimental site

From August 2016 to October 2018 (26 months), 59 tubular P-MFCs were installed in a constructed wetland just south of Budel in Brabant, the Netherlands (51°14′22.5"N 5°35′46.8"E). The pilot site was made available by the Nyrstar Zinc factory located next to the research site. The site was a remediated brownfield; a new sand/loam top layer was added in 1999. The site had little plant growth at the start of the experiment (Fig. 1); it was dry land where the groundwater level was artificially maintained at -3m below the surface. A 1m-high levy was constructed enclosing an area of 8m by 50m. This wetland was fed with water from a small ditch next to the site (unnamed: 51°14′22.0"N 5°35′45.2"E) using a sump pump. A level logger (relative pressure logger, mini-diver Royal Eijkelkamp soil and water, the Netherlands) was connected through Labview using a NI DAQ (USB-6289, National Instruments USA) board that was also used to control a relay to turn the water inlet pump on or off. The pump and level logger were programmed to maintain a 15 cm water layer (above the surface) within the constructed wetland. No maintenance was performed, such as mowing, and no plants were planted or seeded.

2.2. P-MFC assembly and installation

A benchmark tubular P-MFC was used for comparison. The benchmark tubular P-MFC has often been used in pilot and demonstration studies carried out (Patent # EP3167506A1) [38] by Plant-e BV and is also described in the study from Sudirjo et al. [24]. The benchmark tubular P-MFC was a silicone tube (VQM silicone, 12/16 mm inner/-outer diameter, rubbermagazijn.nl, Zoetermeer, the Netherlands), which acted as an oxygen diffusion layer. A layer of carbon felt (thickness 5 mm, size: 100 × 10 cm, KFA-5mm SGL-Carbon GmbH, Bonn, Germany) was wrapped around the cathode. Another layer of the same carbon felt was added as an anode, and the two electrodes were separated by a nonconductive layer made from filter cloth (air filter cloth DA/290, 100 × 19 cm, DACT Filter & Milieutechniek, Kerkrade, the Netherlands). Titanium wire (grade 2, 0.5 mm, Titaniumshop BV, Kampen, the Netherlands) was individually wrapped around the anode and the cathode as current collectors. The tubes were buried about 30 cm in the ground using a trench digger and shovel, submerged well below the water level, which was controlled at 5 cm above the soil surface. The P-MFC was not inoculated with EBSs or other microorganisms. As mentioned above, no plants or seeds were added. The natural biome, i.e., the (microbial) species which lived in or gained access to the location during the experiment were responsible for developing the tubular assembly into an actual P-MFC. This approach was similar to an earlier study that introduced a non-inoculated fuel cell into a laboratory-based constructed wetland where a bioanode and apparent biocathode evolved using natural available microorganisms [23]. The silicone tubes stuck out and were exposed to the air so fresh air with oxygen could flow through and diffuse to the cathode. U-shaped caps were placed on both ends of the tubes to prevent rain from seeping in and were dimensioned so as not to obstruct airflow. Both titanium wires were connected to a copper wire above the water level to prevent corrosion. The connection was made using two different types of heat shrink tubing; the two wires were first physically connected with heat shrinkable solder sleeves, after which a second layer of heavy duty heat shrink tube was added for additional protection. The copper wires were connected to a data collection system (Ni DAQ, USB-6289, National Instruments USA) and through hole resistors that could be manually exchanged (see S5 in the supporting information for the exact resistor values used). A gel-type 3M KCl Ag/AgCl reference electrode (QIS, Oosterhout, the Netherlands) was installed on top of each tubular P-MFC and perpendicular to each anode to measure anode and cathode voltages.

Fig. 1. A: Situation, six months into the test: fully submerged but with little vegetation. B: Situation, 24 months into the test, two months before the site was dismantled. Other than keeping the wetland under waterlogged conditions, no maintenance was performed, nor were any plants planted or (artificially) seeded. C and D: Two of many examples were wetland plants growing in the anode, in this case, Typha latifolia & angustifolia (cattail). The pictures were taken after 26 months, when the pilot site was dismantled.

Different design parameters were investigated and compared, including anode thickness, electrode material, and tube length, as well as a negative control without plants growing. The different parameters are summarized in Table 1. The numbers in the table refer to the location of the tubular P-MFC on the site plan shown on Fig. 2. Data acquisition for one of the #18 triplicates worked fine, and since the configuration was like that of the benchmark, data from this P-MFC was used in the temperature analysis described in Fig. 3.

Table 2 shows the different electrode materials used and the parameters that were changed. For the electrode, carbon-based materials have been used for their conductivity and inertness. Carbon-based felt materials were used for the electrode, the only two exceptions being Ti wire and graphite strips. In this study, two different brands of carbon felt were used: SGL-Carbon GmbH, Bonn, Germany; and Mersen, La Défense, France. The precursor was either PAN (or Polyacrylonitrile), which is synthesized, or Rayon, which is a broad term for many types of natural polymer fibrous material that are used as precursor felt. Different temperatures indicate the temperatures used to carbonize or graphitize the cloth. In the column "treatment," additional steps are mentioned if they were applied anywhere in the production process to further clean, purify or alter the material to meet certain criteria. In the purification step, an inert gas is sent through the material while it is still hot, to drive out any gaseous impurities. Further details on the purification step, as well as "battery grade," KFD and KFA, are confidential information from the manufacturer and were not shared.

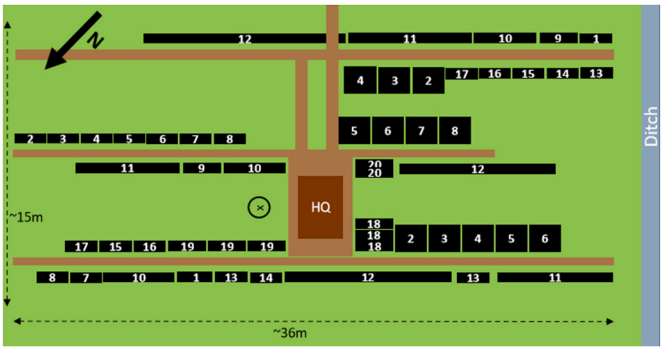

Fig. 2. Schematic plan of the pilot site and installed tubular P-MFCs. HQ (headquarters) refers to the small shed that contained the data acquisition equipment. A water level sensor was installed at the "x" in the circle to control a pump that maintained the water level at 5 cm above the ground. The brown lines mark the installed walkways, ensuring that dry feet when working on the site. The numbers refer to tubular P-MFCs (see also Table 2). Note that tubes 16 and 19 are not included due to technical malfunction.

2.3. Measurements and calculations

The recording of P-MFC cell voltages, anode, and cathode potential, as well as water level and temperature, was performed using a USB multifunctional I/O instrument from national instruments (NI USB-

Table 1
Summary of the different parameters that were changed in this experiment compared to the benchmark tubular P-MFC. The parameters in bold were altered compared to the P-MFC benchmark. The tube numbers correspond to the numbers on the map that indicate the position of the different tubes in the location of the site. The electrode type refers to the numbers that can be found in Table 2, where the different types of electrode materials used for both the anode and cathode are summarized.

TUBE #	TESTED VARIABLE	REPETITIONS	DEPTH (CM)	ELECTRODE TYPE	LENGTH (M)	ANODE THICKNESS (LAYERS)	REMARK
1	–	2	30	1	1	single	benchmark
2	electrode	3	30	**9**	1	single	
3	electrode	3	30	**3**	1	single	
4	electrode	3	30	**2**	1	single	
5	electrode	3	30	**4**	1	single	
6	electrode	3	30	**5**	1	single	
7	electrode	3	30	**6**	1	single	
8	electrode	3	30	**7**	1	single	
9	length	2	30	1	**2**	single	
10	length	3	30	1	**4**	single	
11	length	3	30	1	**8**	single	
12	length	3	30	1	**12**	single	
13	electrode	3	30	**8**	1	single	
14	anode thickness	2	30	1	1	**double**	
15	depth	2	**60**	1	1	single	
17	Blanc	2	30	1	1	single	**without plants**
18	–	3	30	1	**2**	single	**2m benchmark**
20	depth	3	**60, 40, 30**	1	**2**	single	**on top of each other**

Table 2
Different electrode materials used in this study, sorted by parameter.

TUBE #	TYPE	BRAND	PRECURSOR	THICKNESS (MM)	TEMP (°C)	TREATMENT
1	felt	SGL	PAN	5–6	n.a.	KFD
2	felt	SGL	Rayon	5	n.a.	KFA
3	felt	Mersen	Rayon	6	900	purified
4	felt	Mersen	PAN	6	2000	batt grade
5	felt	Mersen	Rayon	6	2000	
6	felt	Mersen	PAN	10	900	purified
7	felt	Mersen	PAN	3	900	batt grade
8	Ti wire	Titaniumshop BV	–	D = 0.5	–	grade 2
9	graphite strips		–		–	

6225, National Instruments, Texas USA) in combination with NI LabVIEW software. The installed water level logger (relative pressure logger, Mini-diver Royal Eijkelkamp soil and water, the Netherlands) that was used to control the water level included a temperature sensor. The temperature of the level logger (relative pressure including temperature logger, Mini-diver Royal Eijkelkamp soil and water, Giesbeek, the Netherlands) (and therefore water body) was recorded throughout the experiment. These temperature values were taken to investigate the effect on the performance of the tubular P-MFCs; the level logger was installed in a drainage tube at 30 cm depth, where the P-MFCs were buried at 20–30 cm below the ground in the same groundwater. Voltages and temperatures were recorded with hourly intervals.

No resistors were connected when new tubular P-MFCs were installed, leaving them in open cell configuration. Three months after the tubular P-MFCs were installed, the voltage was stable, and a first resistor was connected. The current was evidently able to flow in the P-MFC when the resistor was connected, resulting in a drop in cell voltage that often took a few weeks to a few months to stabilize. This behavior is often observed in P-MFCs with (activated) carbon cloth electrodes and is allocated to capacitive currents due to the large surface of the electrode material [39]. Capacitive current is stored and temporary, so to determine the continuous and long-term performance, the capacitive current should not be included. Therefore, the external resistors were replaced when a voltage plateau was reached (<15 mV difference per week), and therefore the current stabilized.

To smooth out the zigzags that form during a trend formation (signal to noise) and better visualize actual trends, running averages were calculated using subsets of 30 data points. Averages and standard deviations were calculated using data from triplicates per parameter. Markers were added in some graphs to further clarify the differences between lines. The markers, when included, are no additional data points but are visualized every 504th data point, an arbitrary interval that was chosen for visual and clarity reasons. The complete data set used is provided as a courtesy from Plant-e BV, the Netherlands, and can be provided on request. Currents were calculated using Ohm's law from external resistor values and recorded cell voltages. (Equation (2)). Multiplying the current by the corresponding voltage resulted in the power produced by the system (Equation (1)).

$$P = U * I \quad \text{(eq. 1)}$$

$$I = \frac{U}{R} \quad \text{(eq. 2)}$$

Where I is the current (A), U the voltage (V), P power (W), and R the external resistance applied (Ω). The cell potential is defined by the difference between the cathode and the anode potential (Equation (3)).

$$U_{cell} = U_{cat} - U_{an} \quad \text{(eq. 3)}$$

Ionic losses can be expected because of the distance between the electrodes. In this research, total losses through dissipation as well as ohmic losses attributed to ionic resistance and material resistance are included. The total loss was calculated by determining the total potential drop of the P-MFCs at any given time, using Equation (4). The ohmic loss attributed to ionic resistance is a function of the voltage drop ΔU_{ion} (V) that was calculated using Equation (5). In this study, an equivalent circuit is proposed to determine the ohmic loss through the resistance of the material. A detailed explanation of the method used for the resistance of the material can be found in S1.

$$\Delta U_{tot} = U_{OCP} - U_{cell} \quad \text{(eq. 4)}$$

Where U_{OCP} is the highest cell potential (V) measured when the P-MFCs were in open circuit. U_{OCP} was obtained during the first three months of the experiment allowing the Plant-MFC to stabilize in a new redox environment. U_{cell} is the cell potential (V) measured at any given moment.

$$\Delta U_{ion} = \frac{dj}{\sigma} \quad \text{(eq. 5)}$$

Where d = distance between electrodes (cm), j = current density (A/cm^2) and σ = conductivity (S/cm) [39,40].

To determine the long-term maximum power, and to eliminate the seasonal influence on the P-MFC, polarization curves were obtained after the tubular P-MFCs were removed from the test site and placed in an indoor bin. Four tubular P-MFCs were selected–one control tube (#1) and three tubes with a different electrode material (#7, with electrode material 6)–to see whether the behavior was different. The containers were kept at room temperature (20° C) in sediment sludge taken from a nearby ditch (not analyzed), and the level of water was maintained above the surface by manually watering the containers. Power production is normalized to the production per projected plant surface to be able to compare it with other studies in the literature. The projected plant surface is the area in square meters that is occupied by the tube on the surface, looking from the top.

3. Results & discussion

3.1. Long-term performance: significant effects of temperature, seasons, and plant growth on the P-MFC

In this study, a plant-rich wetland was established without actively introducing plant species. The plot of the original brownfield had little visible original vegetation. Keeping the soil permanently covered with 5 cm of water from the nearby ditch throughout the experiment resulted in a clear increase in vegetation compared to the soil outside the constructed wetland. Biomass quantification was not performed, but visual evidence leaves no doubt, as can be seen in Fig. 1A and B. The origin of the increased flora is not precisely known; seeds could have been transported through the air or through wildlife (like birds) or been pumped in through the pumping installation that was used [19]. Another option could be that seeds and/or much smaller vegetation were present before the constructed wetland was created that started to flourish after the land was permanently flooded. At the end of the project, all tubular P-MFCs were dug up and inspected. Fig. 1C and D shows some examples of many tubular P-MFCs that had roots growing into the anode felt. Plants sometimes even germinated from the tubular

Plant-MFCs. Plant species that where most dominant and visible in the constructed wetland where species present in Dutch natural areas, i.e., *Typha latifolia & angustifolia* (cattail) and *Equisetum fluvatile* (water or swamp horsetail).

Electrical energy was generated by the installed P-MFCs that were exposed to changing environmental conditions such as temperature, plant growth, and rainfall. Both the air temperature and the temperature observed at 30 cm below the surface changed with seasons (see S3). None of the tubes investigated experienced day-night temperature fluctuations as shown before by, e.g., rooftop P-MFCs [41], likely because they were buried 30 ± 5 cm below the surface and water level, limiting the effect of air temperature dynamics (see S3). The tubular P-MFCs were exposed to groundwater at the anode and ambient air via the gas diffusion tubes at the cathode. The temperature that the P-MFC experiences is assumed to be similar to the water at that depth, because the heat capacity of air is $3.5*10^{-6}$ lower than the heat capacity of water [42], making it much easier for water to transfer heat and therefore influence the temperature of the P-MFC. The lowest-observed temperature to which the tubular P-MFCs were exposed was 4.0° Celsius in mid-February 2017. The highest-observed temperature to which the tubular P-MFCs were exposed was 19.5° Celsius in mid-August. At lower temperatures, a higher anode potential was typically observed and vice versa, indicatively shown in Fig. 3 (data is collected from two groups of P-MFCs: #1 benchmark and #18 right behind each other; both groups consist of the same type of P-MFCs, with the exception that the latter is 2m and the control 1m long, for fourteen months, from August 2017 to October 2018). The cathode potential remained relatively stable, between 200 and 500 mV vs. Ag/AgCl throughout the season. Cell potentials in winter (December to February, water temperature between 5 and 10° Celsius) were often less than 50 mV (November to May) and current production in winter (<0.35 mA) was also lower than in warmer summer (June to September, water temperature between 17 and 21° Celsius) (1.3–3.35 mA).

3.2. Incoherent P-MFC vs. Temperature correlation between spring and fall

In this study, the current production of tubular P-MFC was compared with soil temperature to understand if a correlated temperature relationship is present under the tested wetland conditions. The anode and cell potential seem to follow the temperature trend, but with a several weeks to months lag (Fig. 3). Cell potential drops in winter with an increase in anode potential. The cathode potential shows evidently less variation than the anode potential throughout the different temperatures, varying between 300 and 550 mV vs. Ag/AgCl (see S8). Some studies found the oxygen supply to be limiting, resulting in lower cathode potentials [4], but in this study the more stable and positive cathode potential suggests the oxygen supply was not limiting the current production of the tubular P-MFC. The temperature data in this study suggest a significant drop in current production when comparing production at 12 °C and 5 °C, with a sharp decrease from 6.5° Celsius and below (Fig. 4). The data is collected from a random selection of P-MFCs that had similar anode material: #1 benchmark; #14 thick anode; #17 no plants; #20 twice normal depth, all showing a similar pattern (individual data sets can be found in the S7). When the temperature drops below 6 °C, the average current production drops faster: there is a quasi-linear drop that describes the average current for temperatures above 6 °C with a gradient of 16 μA/°C of current loss per degree Celsius. Around the 6 °C mark, the gradient is steeper with 55 μA/°C of current loss per degree Celsius. Although there is variation in the data, there is a significant difference between the current production at 12 °C and 5 °C, supporting a correlation between outdoor temperature and average current.

There are several temperature-dependent processes happening in the anode of a P-MFC that can cause an increase of the anode potential. First, current is naturally generated at the anode with microorganisms that are temperature sensitive [27,43]. The metabolism of EAB will slow down at lower temperatures, resulting in a lower current production. Diffusion of substrate for microorganisms is also affected by temperature and will

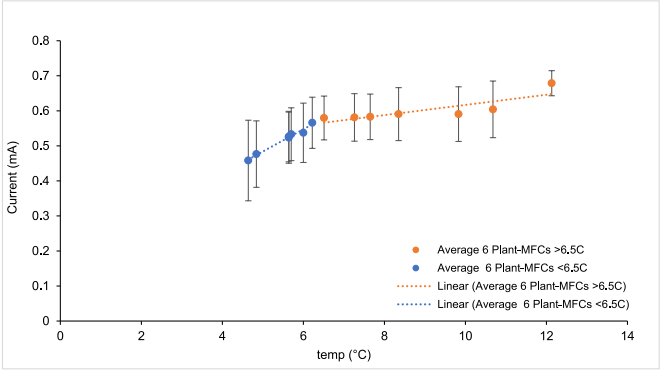

Fig. 4. Correlation between current production and water temperature 30 cm below the surface, to which the P-MFCs were exposed. Data from random selection of P-MFCs that had similar anode material: #1 benchmark; #14 thick anode; #17 no plants; #20 twice normal depth and gathered between October 2016 and February 2017: five months.

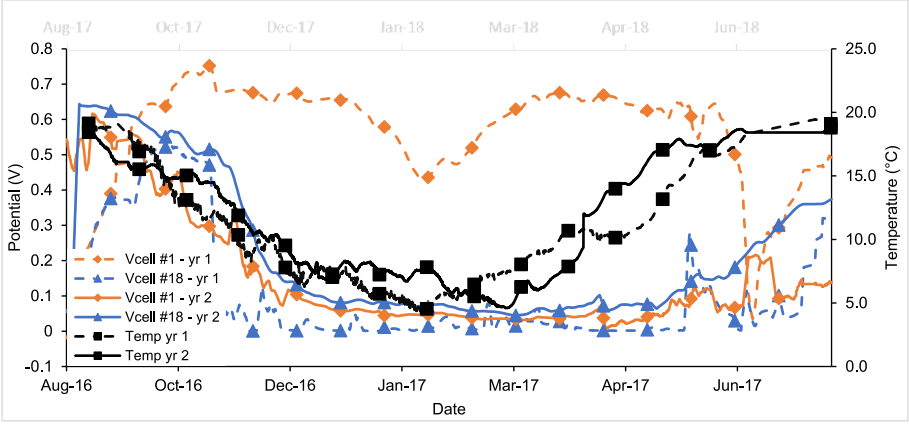

Fig. 3. Fluctuations in cell potentials throughout the season, following the temperature fluctuation, but especially in the spring, there is a visible delay. Vcell #1-control managed to maintain a high cell potential during the first year of operation, including the winter, while dropping significantly during the winter of the second year. The large and sudden dip of Vcell #1 control year 1 in June 2017 can be explained by a pump failure, leaving the constructed wetland dry for a short time. The markers are existing data points visualized as markers every 504th data point (an arbitrary value) and act as additional visual clarification.

slow down with lower temperatures as described by the Einstein-Smoluchowski-Sutherland relation [44]. The internal resistance of the P-MFC is, among other things, determined by the diffusion coefficient of ions in the solution [39]. The diffusion coefficient of ions in solution is also affected by temperature; hence, a lower temperature will increase the internal resistance of the P-MFC system. Finally, the chemical reaction rate constant is temperature dependent according to the Arrhenius equation [45], meaning the reaction rates will go down with lower temperatures, both at the anode and at the cathode.

This study shows the temperature correlation; for example, the anode potentials rise when the temperature drops, but this effect fluctuated throughout the different years, as can be seen in Fig. 3. Seasonal temperature trends were comparable throughout the two years, but cell potentials did not follow the temperature fluctuations consistently, suggesting that other processes play a role. Group #1-Control had a high cell potential during the winter of the first year, for example, but dropped in the second winter. In the fall, the cell potential drops as the temperature drops, but in spring there is a delay of two to three months between the trend of increasing temperature and the increase in cell potentials (Fig. 3). Since the cathode potential was stable throughout the year, the changes are the result of a rising anode potential. The anode potential is affected by the water chemistry, such as pH, dissolved molecules, substrate availability, etc. These conditions could have been different between years because the water used to feed the constructed wetland was pumped from a ditch that farmers also used in the neighborhood. Farmers can use pesticides or fertilizers, which could end up in the ditch through run-off, resulting in for example different amounts of nitrate, which is considered to be an alternative electron acceptor [26] and therefore lowering the coulombic efficiency.

Another reason for seasonal fluctuations could be the interaction of plants with the P-MFC. Two wetland plants that were found predominantly in the constructed wetland were *Typha latifolia & angustifolia* (cattail) and *Equisetum fluvatile* (water horsetail). Both plants are known for their ability to transport oxygen down into the rhizosphere [46,47], were much more abundant as the pilot progressed, and were frequently found growing in the anode, with roots and rhizomes. In springtime, plants grow fast and have a high metabolism and photosynthetic activity. These processes are related to increased transportation of oxygen to the root system [48]. Oxygen is an alternative electron acceptor and facilitates aerobic microbial activity, lowering the coulombic efficiency of the P-MFC [49]. The delay between the temperature change and the cell potential going up observed in spring may therefore be related to oxygen transport into the anode by plant roots.

Finally, root exudation and rhizodeposition can play an important role in the performance of P-MFCs [50,51]. As plants grow, they release organic matter such as rhizodeposits and plant litter that can be converted by EAB [3,52]. There is evidence suggesting carbon excretion by plant roots also varies with temperature [53,54], where lower temperatures result in less carbon through root exudation and therefore a lower carbon availability in the anode, resulting in less current. Many roots were found to be growing in the anode part of the tubular P-MFCs when disassembling the pilot, which would support the hypothesis on the effect of exudation and oxygen release. In this research, a series of blank tubular P-MFCs was investigated to test this hypothesis. This blank tubular P-MFC was shielded from plant growth and surprisingly performed similarly to the benchmark tubular P-MFC. Unfortunately, the variability in the blank series was too high to draw conclusions, but it seems to suggests that other mechanisms, such as variability in biological activity or substrate, are involved in explaining the dynamic performance over time (data can be found in S4, not shown due to high variation between replicates).

3.3. P-MFC tube length and its effect on electricity generation

In this study, the longest P-MFCs made so far were evaluated based on performance. The length of the tube influenced the current and thus the power production of the P-MFC, which was assessed for a period of twenty weeks. The performance of the tubes with a length of 1, 2, 4, 8, and 12 m is summarized in Fig. 5.

Longer tubular P-MFCs seemed to produce more power, but due to the large variation between the replicates, it is not possible to show significant differences (see Fig. 5a, data set on the left side). Only the difference between the 1m and 8m tubes is significant, and the 8m tube performs better. If the charge and energy production are normalized to production per meter tube (see Fig. 5a, data set on the right side), however, the 2m tubes produced the most current (i.e., charge transfer) and energy. Although smaller, 1m tubes produced similar amounts of energy per meter as compared to the 2m tubes and can therefore be recommended for effective material use.

The lower relative energy production and charge transfer observed (see Fig. 5b) can be explained by various aspects including differences in biofilm configuration, oxygen transport to the cathode, local variations and soil conditions, different ohmic losses, and, finally, local differences in pH [55], but pH was not measured throughout the experiment.

Longer tubes provide more total surface area for EAB to grow, resulting in higher energy production. A possible reason for the differences in energy production with length could be the biofilm size; a larger biofilm can indicate more current production as well as a change in internal resistance. There have been several studies that looked into the conductivity of *Geobacter-type* biofilms, where metallic-like conductivity was sometimes found [56] and sometimes biofilm conductivity was found that was several orders of magnitude lower [57]. After the tubular P-MFCs in this study were dug up and inspected by eye, no visual (differences) in the biofilm covering were observed. It seems like there is no evidence from the field or the literature that can quantitatively relate EAB occurrence to differences in normalized performance between the different P-MFC lengths.

Longer tubes will also result in a longer distance between fresh oxygen from the air and the cathode where it is used. Oxygen is reduced at the cathode and naturally diffuses into the tube from the two openings on either side. As oxygen is consumed, the concentration will drop, which can become a rate-limiting step. As the tubular P-MFC becomes longer, the oxygen must be transported over a larger distance, which can lead to limitations in current production. Wetser [58] calculated the maximum length of a P-MFC based on a theoretical model based on oxygen diffusion and concluded that oxygen becomes limiting when tubular P-MFCs are longer than 0.77m [58]. However, the stable positive cathode potential observed in this study suggests that the oxygen supply was not limiting the current production of the tubular P-MFC even at lengths of 12 m. One reason for this difference could be convection, which was not considered in the approach of Wetser et al. Because this study is carried out outside where the air will often not stagnate, convection can increase the oxygen refreshment rate within the tubular P-MFC. The second reason could be the lower current production observed in this field study: with the limited current produced by the EAB, limited oxygen needs to be supplied to the cathode. Wetser found that the best performing P-MFC under laboratory controlled environmental conditions was 1.3 mA/m, where in this study the 12m tubular P-MFC produced on average 0.2 mA/m, with a maximum observed value of 0.7 mA/m, a factor of 7 to 5 lower (see S6). With a lower current density, the maximum tube length before oxygen will be limiting can also be increased by the same factor.

Longer tubes include more materials than shorter tubes, resulting in a different internal resistance, which affects the performance of the P-MFC. Fig. 6 illustrates the estimated losses in the P-MFCs with different lengths, split for totals, and normalized values (per meter tube). Different losses were calculated to investigate whether differences in internal resistance could explain the difference in relative performance. The internal resistance was further specified as material resistance and ionic resistance. When the tubes are longer, more electrode and current collector material is used through which the current flows. With more material used, total internal resistance also increases [59,60], by

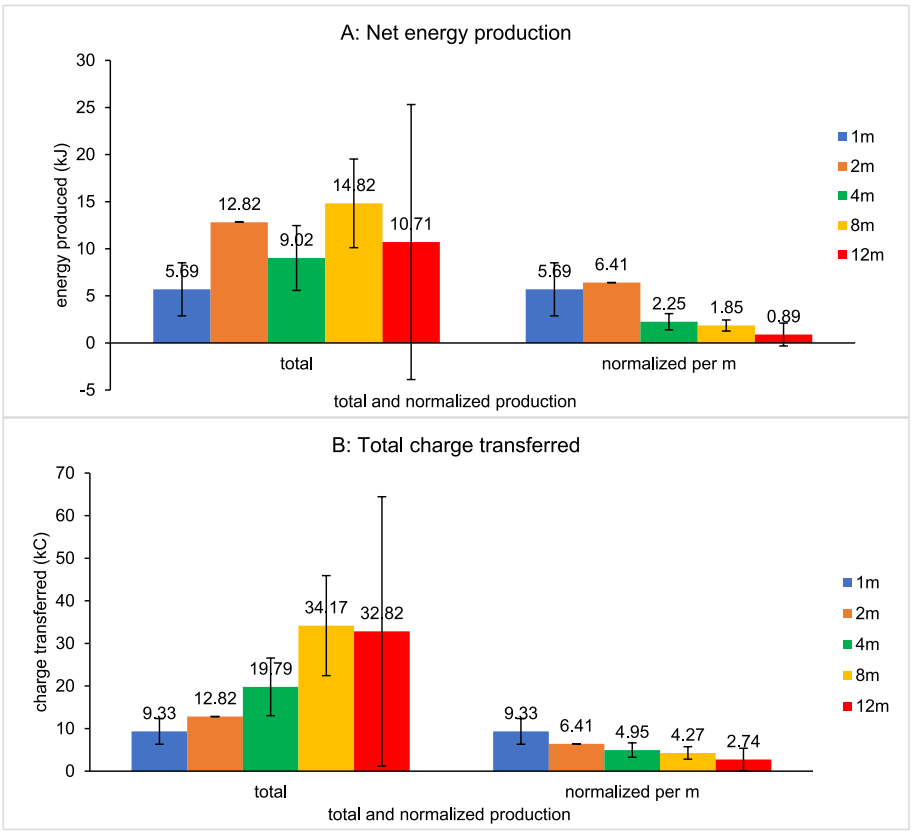

Fig. 5. performance of the tubular P-MFC systems of five different lengths. Figure A shows the total energy produced over twenty weeks (April 5, 2017 to August 24, 2017) and the total energy produced per meter tube (normalized production). Figure B shows the total charge transferred over the same twenty weeks and also the total charge transferred per meter tube (normalized). Repetitions for 1m: n = 2, 2m: n = 1, 4m: n = 3, 8m: n = 2, 12m: n = 3.

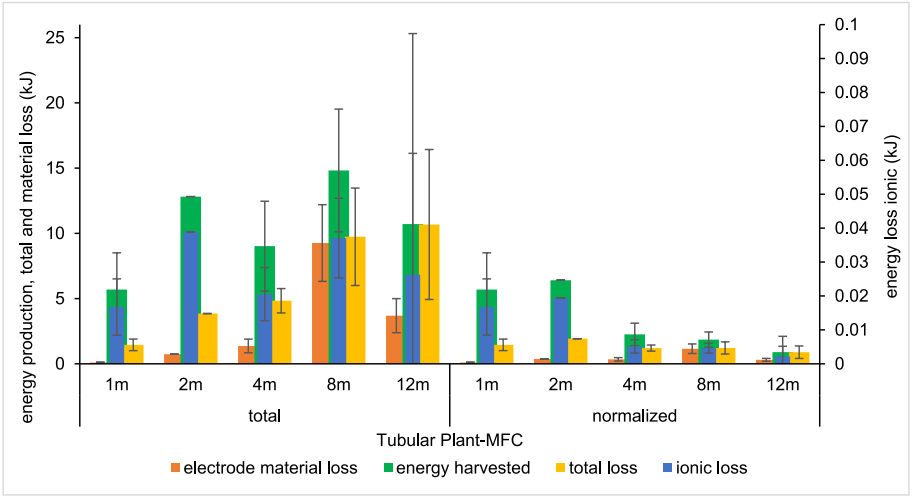

Fig. 6. Energy harvested by tubular P-MFC systems of five different lengths: the relationship between the theoretical losses calculated through material resistance, based on the current and specific properties of the material (see S1 for the method used), through ionic losses compared to the energy harvested. Mind the different scale for the ionic loss on the right axis.

increasing losses mainly through electrode material and interconnections. In this study, an equivalent circuit is proposed to determine the total resistance of the material through the current collectors and the anode/cathode electrodes of the different tubes. A detailed explanation of the method used to determine the resistance of the material can be found in S1. Furthermore, the estimated ionic loss, which expresses the resistance of ions to migrate between the electrodes, was calculated by Equation (5) described in the Materials and Methods section. The results show that the ionic losses were minimal and contributed to a maximum of 1.1 % of the total energy loss.

The energy losses due to material resistance were especially significant for the 8m and 12m tubes, where 56 % and 57 % of the energy production was dissipated through losses. Although the energy harvested in these larger systems is lower, it only explains part of the difference in relative power production that was observed as the tubular P-MFC grew longer. There are more studies that have found that upscaling

the electrode material in a MFC system can lead to a lower relative power production [61,62,63], but this is the first time it has been observed in a P-MFC.

3.4. Non-significant effect on average electricity generation due to different electrode types

In this study, several P-MFCs with different commercially available materials as electrodes were investigated. Seven different types of cloth were tested, as well as tubular P-MFCs without a true electrode, where titanium wire or graphite strips doubled as an electrode and current collector in one. Finally, a negative control was included, where the root cloth prevented the plants from growing in the electrode material.

The results of the material test are presented in Fig. 7, showing the net energy and charge produced during 170 days of operation, from April to September 2017. The benchmark P-MFC produced 1.96 kJ of energy and transferred 8.03 kC of charge during this time. The tubular P-MFC that was shielded from plant growth but buried in the same soil was not significantly different from the P-MFCs that were exposed to plant growth, but the variation between the duplicates was large. Making the anode double as thick with the same electrode material as was used for the benchmark did make a significant difference and produced more charge and electrical energy. The tubular P-MFCs without an electrode (Ti wire and graphite strips) did not show notable current or negative (reversed) current and power production over a one-year operation, illustrating the need for the carbon anode and cathode electrode. On average, the *Mersen PAN 2000C no purificat*ion 6 mm battery grade and Mersen PAN 900C 10mm outperformed the benchmark tubular P-MFC by up to 180 %.

Although seven different cloth types were used, the difference in energy output and charge transfer was limited; only two types of material outperformed the benchmark, but there is no common denominator between these two. The two tubular P-MFCs that only had a current collector installed, but no electrode, performed significantly worse. It seems that a large electrode surface is necessary to generate electricity and support EAB in generating electrons.

The tubular P-MFCs with a double-thick anode performed better than the benchmark, by 17 % on average. Although the anode in the benchmark was the limiting factor, doubling the thickness of the anode and effectively also the surface of the cloth, the current and energy production did not double. A larger electrode surface means more space for the EAB to populate the electrode. More EAB can result in a thicker biofilm and consequently more current and energy production, although this can lead to pH gradients and substrate diffusion limitations within the biofilm [64,65]. In particular, the pH gradient within the biofilm will start to inhibit current production of the EAB when current densities will be 5A/m^2 or more [55,66]. However, in these studies, high current densities are achieved with high substrate concentrations in the bulk, under well-mixed conditions. Although substrate concentrations were not measured in our study, wetland and soil concentrations of readily available substrate are typically much lower than the concentrations used in laboratory studies. In addition, the current density is much lower (20 mA/m^2 in this study, a factor of 250 lower), indicating that the electrode surface is not the limiting factor, supporting the hypothesis of limited substrate availability from the bulk. Since the Plant-MFCs are buried in the subsurface, little mixing occurs, and the availability of soluble organic matter is low [4], it seems likely that diffusion limitations occur in transportation of the electron donor to the anode (biofilm). Therefore, substrate limitations from the bulk, and/or local pH or substrate gradients in the biofilm can explain why the double-thick anode did not perform twice as well as the benchmark. Finally, a thicker electrode will increase local transport and ionic resistances, which will also reduce the energy recovery. Therefore, using less material for the electrode seems to be a valid strategy to save material use and associated costs while having an acceptable reduction in power production.

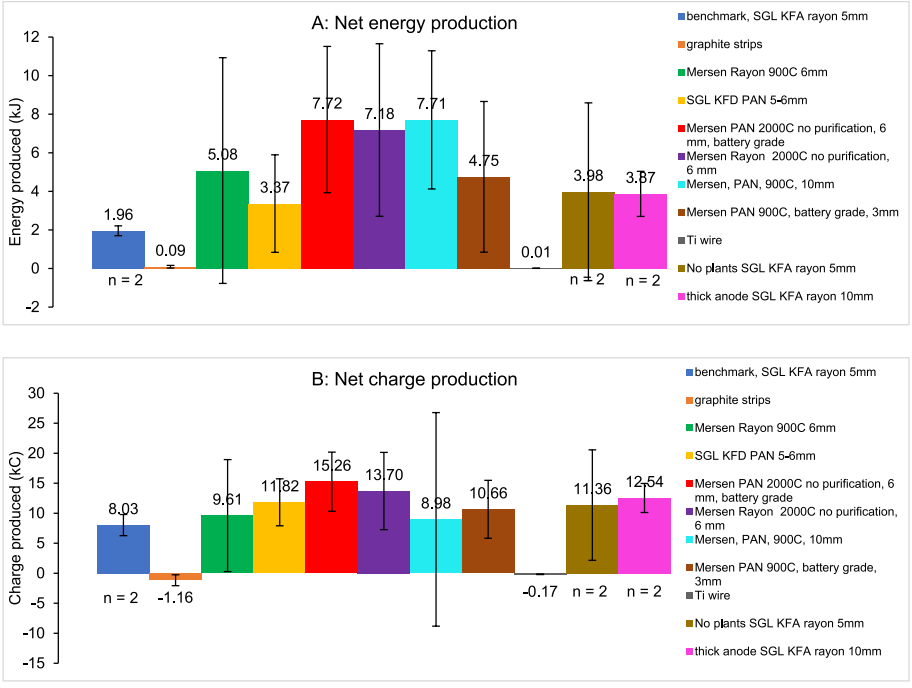

Fig. 7. A: Energy and B: Charge production of nine different electrode materials, produced in 170 days operation from April until September 2017. Tubular P-MFCs where the electrode was left out and only had a current collector from titanium wire or graphite strips produced insignificant amounts of energy and charge. All standard deviations are the results of tests in triplicate except for the benchmark, the blank, and the thick anode, which were done in duplicate and are marked with "n = 2" in the graphs.

3.5. Long-term maximum power production with long-term polarization curves

In this study, four tubular P-MFCs were selected to perform polarization curves: one control tube (#1) and three tubes with a different electrode material (#7, with electrode material 6), to see if the behavior was different. The "long-term" maximum power was estimated and not a short-term maximum power of, for example, minutes/hours as is often used in other studies [67,25,68]. This was done since longer waiting times are needed in order to minimize the capacitive current effect, also described by Ref. [39]. To eliminate the effect of temperature on the potentials and current production on the P-MFC, polarization curves were obtained after the tubular P-MFCs were removed from the test site and placed in a bin indoors.

The polarization curve showed a typical shape that is observed more often with P-MFCs where the current production drops significantly after the maximum power point is reached [39]. The maximum power point was found when applying a resistor of 330 Ω (Fig. 8), corresponding a maximum power point between 0.9 and 1.3 mW at potentials between 0.55 and 0.65V, or 13–18 mW/m^2 projected plant surface, which is twice as high as a comparably-designed P-MFC used in a rice paddy in Kalimantan, Indonesia [24]. The potential drop at MPP was only 25 % compared to the open cell potential, which is lower than observed in typical Plant-MFC and MFC studies [67,51,69–71]. The configurations of the systems used in these studies are different, so it is hard to compare the polarization curves [24]. used a comparable design as is used in this study, but the polarization is done in much less time (hours/min) than in this study (months), overestimating the long-term maximum power production [67]. The final load step, between 330 and 150 Ω, resulted in a sharp potential and current drop, and consequently the power production was reduced by 65 %. The polarization curves generated in this study provide guidance in power harvesting strategies when using tubular P-MFCs. The voltage is well maintained when drawing more current until a sharp drop manifests shortly after the MPP, so it seems advisable not to harvest close to the MPP.

3.6. Toward applications: using performance characterization to develop harvesting electronics and future work

When using the P-MFC as a power source, an electronic harvester board is connected to harvest the electricity from the P-MFC and increase the voltage from the P-MFC to voltages suitable for small applications with minimal conversion losses. Ideally, this harvester can be programmed so that it harvests electricity at a potential that corresponds with the potential at the systems maximum power point (MPP) [72]. In this way, the maximum power can be harvested. The experimental conditions and the explained environmental factors such as temperature, influencing reaction kinetics, substrate availability, and microorganisms all vary and likely influence the shape of the polarization curve, which therefore changes with conditions and time. To overcome this, harvesters can also be equipped with MPP-trackers that monitor the harvesting potential and current development over time and ensure an optimal harvesting regime, even if conditions change [73,74]. To develop a proper MPP harvesting and tracking regime, understanding the shape of the power curve and the behavior of the system as the current is harvested is crucial. The data provided in this research can, therefore, be a valuable contribution to the development of such harvesting electronics. Some studies describe harvesters connected to a P-MFC, working at 3.5 mW/cm^2 [21] or even 2.09 μW [22], and on the same order of magnitude as the power production found in this study. Therefore, it is expected that the tubular P-MFCs used in this study are a suitable power source for low, milliwatt power electrical applications in the field, although backup and electrical buffer capacity should probably be included for ensured operation at lower temperatures and temporary unfavorable soil and or plant conditions.

This study has shown that long-term studies under outdoor conditions can be challenging, mainly due to the large variation in the data that are collected. Furthermore, different wetland plants and different environmental or climate conditions can influence performance, and more insight into these factors can create the boundary conditions for the application of the P-MFC. In conducting such tests, a larger number of repetitions than three would be recommended to reduce variability. Furthermore, the quantification and qualification of plants that grow in the wetland system over time can provide a correlation between the performance of P-MFC and the development of certain species. Finally, a thorough microbial analysis on the soil, in particular close to and in the electrodes of the P-MFC, can provide insight into the role of different microorganisms on the performance of the P-MFC, although such work has been done by Sudirjo et al. [24] with a similar system, who did not find clear differences between the microbial community inside the electrodes, and that a few meters away.

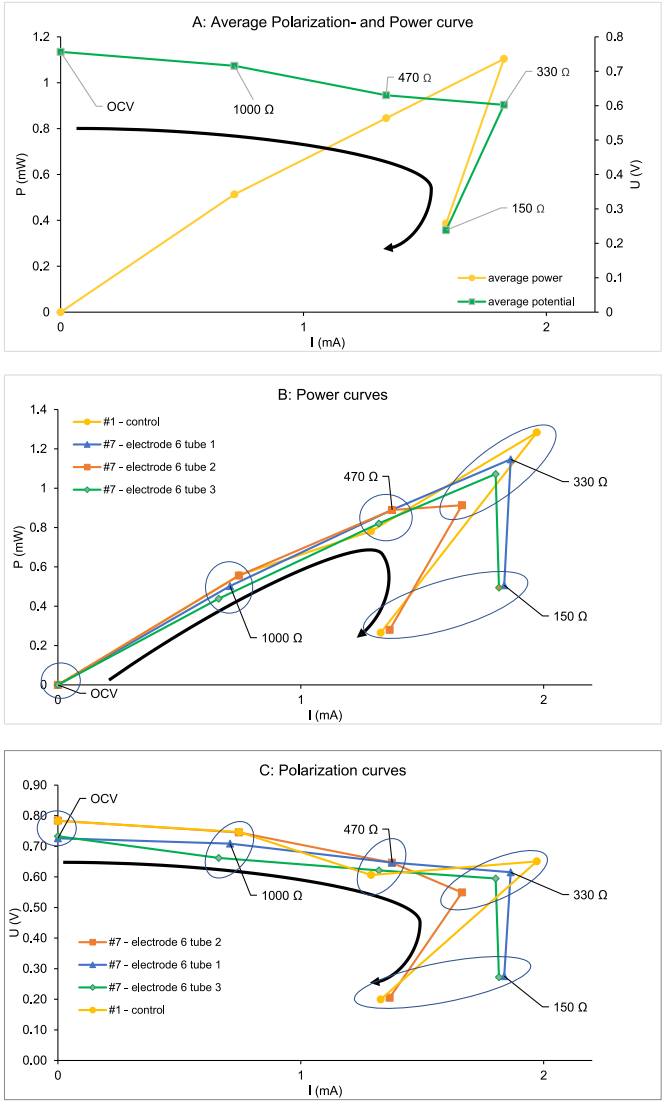

Fig. 8. Polarization and power curves of four tubular P-MFCs. The interval between the change of the resistor has been chosen carefully to eliminate the influence of the capacitive current. It took on average two months (data not shown) between the resistor changes; the next resistor was connected only when the voltage had stabilized at the then applied load. The black arrow indicates the chronological order in which the resistors have been changed. Figures B and C show the power and polarization curves of the individual tubular P-MFCs, where the colors correspond with individual P-MFCs. Figure A shows the average, using the same data as was used for Figures B and C.

4. Conclusion

P-MFCs were successfully installed in a constructed wetland, created on a brownfield at pilot scale. A maximum production of 13–18 mW/m^2 was found, which would make the tubular P-MFC a viable stand-alone power source for low-power remote sensing equipment. Long-term monitoring showed variation over the seasons, while performance changed over the years. Temperature seems to correlate with the performance of tubular P-MFCs. The correlated performance of the P-MFC dropped faster at temperatures below 6 °C. In winter times, the power production drops by up to 90 %, so in low-temperature regions a backup battery could be necessary. Longer tubular P-MFCs produce more power, but do not do so when normalized to power per meter, where the optimum seems to be around 1–2 m long. On average the Mersen PAN 2000C no purification 6mm battery grade and Mersen PAN 900C 10 mm outperformed the benchmark tubular P-MFC, by up to 80 %, but there is no common denominator between these two, so there is no clear explanation for the difference in performance. A thicker anode performed up to 17 % better and systems with a current collector alone were not able to produce power. There is probably room for improvement in the design of the P-MFC by using less or cheaper material, since the used design is not very sensitive to different electrode material choices and smaller P-MFCs seem to perform relatively well. Not all fluctuations in energy production over the years could be explained by the investigated variables; there are likely unknown dependencies of plant growth and species as well as soil conditions that influence the performance of the P-MFC. To utilize P-MFC power for sensor applications, an appropriate harvester should be designed that is able to monitor the production capacity of the P-MFC while harvesting and have sufficient buffer capacity when lower temperatures are expected. Similar large-scale pilots, such as the work presented under different circumstances, e.g., different climate and different wetland plants, can provide the necessary data to indicate how reliable the P-MFC performance is, versus under different wetland conditions.

CRediT authorship contribution statement

Pim de Jager: Design of the experiment, Data analysis and interpretation, Drafting the article. **Daniel Groen:** Design of the experiment, Data collection, Critical revision, Support on interpretation. **David P.B. T.B. Strik:** Critical revision, Support on data analysis and interpretation.

Declaration of competing interest

The authors declare the following financial interests/personal relationships which may be considered as potential competing interests:

D. Groen is employed by Plant-e BV, P de Jager is employed by both Plant-e BV as well as the Wageningen University as a researcher. **All authors declare no competing interests**.

Pim de Jager reports financial support and equipment, drugs, or supplies were provided by Plant-e BV.

Pim de Jager reports a relationship with Plant-e BV that includes: employment.

Pim de Jager and David P.B.T.B. Strik are inventors on a patent #WO2015183084A1 issued to Plant-e knowlegde BV.

This research is financed by the Netherlands Organization for Scientific Research (NWO), which is partly funded by the Ministry of Economic Affairs, and co-financed by the Netherlands Ministry of Infrastructure and Environment and partners of the Dutch Water Nexus consortium (project nr. STW 14302 Water Nexus 3). Data-set was a result of a project co-funded by The Province of North-Brabant, the Netherlands: “Grootschalige elektriciteitsproductie met levende planten” (project nr. C2184543/3925942).

Acknowledgments

This research is financed by the Netherlands Organization for Scientific Research (NWO), which is partly funded by the Ministry of Economic Affairs, and co-financed by the Netherlands Ministry of Infrastructure and Environment and partners of the Dutch Water Nexus consortium (project nr. STW 14302 Water Nexus 3). The authors thank Plant-e BV for providing the data set that is used in this study, Maxim Cornelissen for his contribution on the polarization curves, Marjolein Helder and Nora Sutton for their useful comments, and Nyrstar, Budeldorpplein for providing the field location. The data set was the result of a project co-funded by the Province of North-Brabant, the Netherlands: “Grootschalige elektriciteitsproductie met levende planten” (project nr. C2184543/3925942).

Appendix A. Supplementary data

Supplementary data to this article can be found online at https://doi.org/10.1016/j.renene.2023.119532.

References

[1] C. Wardman, K.P. Nevin, D.R. Lovley, ’Real-time monitoring of subsurface microbial metabolism with graphite electrodes’, Front. Microbiol. 5 (2014).
[2] Christopher K. Algar, Annie Howard, Colin Ward, Gregory Wanger, ’Sediment microbial fuel cells as a barrier to sulfide accumulation and their potential for sediment remediation beneath aquaculture pens’, Sci. Rep. 10 (2020), 13087.
[3] David P.B.T.B. Strik, H.V.M. Hamelers, Jan F.H. Snel, Cees J.N. Buisman, ‘Green electricity production with living plants and bacteria in a fuel cell’, Int. J. Energy Res. 32 (2008) 870–876.
[4] K. Wetser, E. Sudirjo, C.J.N. Buisman, D.P.B.T.B. Strik, ’Electricity generation by a plant microbial fuel cell with an integrated oxygen reducing biocathode’, Appl. Energy 137 (2015) 151–157.
[5] Tom H.J. A. Sleutels, Sam D. Molenaar, Annemiek Ter Heijne, Cees J.N. Buisman, ’Low substrate loading limits methanogenesis and leads to high coulombic efficiency in bioelectrochemical systems’, Microorganisms 4 (2016) 7.
[6] Arends, B.A. Jan, Speeckaert Jonas, Evelyne Blondeel, Jo De Vrieze, Boeckx Pascal, Willy Verstraete, Korneel Rabaey, Nico Boon, ’Greenhouse gas emissions from rice microcosms amended with a plant microbial fuel cell’, Appl. Microbiol. Biotechnol. 98 (2014) 3205–3217.
[7] Tianran Sun, Juan J.L. Guzman, James D. Seward, Akio Enders, Joseph B. Yavitt, Johannes Lehmann, Largus T. Angenent, ’Suppressing peatland methane production by electron snorkeling through pyrogenic carbon’, bioRxiv (2020) 2020, 02.15.950451.
[8] Lucia zwart, J. Cees, N. Buisman, David Strik, ’Plant-Microbial fuel cells serve the environment and people: breakthroughs leading to emerging applications.’, in: Deepak Pant Sonia M. Tiquia-Arashiro (Ed.), Microbial Electrochemical Technologies, CRC Press, Boca Raton, 2019.
[9] Zhihao Lu, Di Yin, Peng Chen, Hongzhen Wang, Yuhang Yang, Guangtuan Huang, Lankun Cai, Lehua Zhang, ’Power-generating trees: direct bioelectricity production from plants with microbial fuel cells’, Appl. Energy 268 (2020), 115040.
[10] Janneke Vader, Aris Gaaff, Madeleine van Mansfeld, Willem van Deursen, Renkums Beekdal geopend Effecten sanering en herinrichting voormalig bedrijventerrein, in: Den Haag: LEI Wageningen UR, 2013. Den aag.
[11] UK, Forest research, ’Wetland habitats’. https://www.forestresearch.gov.uk/tools-and-resources/fthr/urban-regeneration-and-greenspace-partnership/greenspace-in-practice/benefits-of-greenspace/wetland-habitats/, 2022. (Accessed 16 June 2022).
[12] Rashmi Sharan Sinha, Yiqiao Wei, Seung-Hoon Hwang, A survey on LPWA technology: LoRa and NB-IoT, ICT Express 3 (2017) 14–21.
[13] D.R. Prapti, A.R. Mohamed Shariff, H. Che Man, N.M. Ramli, T. Perumal, M. Shariff, ’Internet of Things (IoT)-based aquaculture: an overview of IoT application on water quality monitoring’, Rev. Aquacult. 14 (2022) 979–992.
[14] S.M. Mousavi, A. Khademzadeh, A.M. Rahmani, ’The role of low-power wide-area network technologies in Internet of Things: a systematic and comprehensive review’, Int. J. Commun. Syst. 35 (2022).
[15] K. Wójcicki, M. Biegańska, B. Paliwoda, J. Górna, ’Internet of things in industry: research profiling, application, challenges and opportunities—a review’, Energies 15 (2022).
[16] L. Schirone, P. Bellucci, On the quality of photovoltaic-sound barriers, Acta Acustica 89 (2003) S30–S31.
[17] David Parsons, ’The environmental impact of disposable versus rechargeable batteries for consumer use’, Int. J. Life Cycle Assessment - Int. J. Life Cycle Assess 12 (2007) 197–203.
[18] Mahmuda Mishu, Md Rokonuzzaman, Jagadeesh Pasupuleti, Mohammad Shakeri, Kazi Sajedur Rahman, Fazrena Hamid, Sieh Kiong Tiong, Nowshad Amin, ’Prospective efficient ambient energy harvesting sources for IoT-equipped sensor applications’, Electronics 9 (2020) 1–22.

[19] Coupland, Alison M. Smith George, Plant Biology (Taylor & Francis Inc: New York). davies, huw. 2021. 'Micro energy harvesting can provide potentially inexhaustible electrical energy captured from the ambient environment, ideal for IoT sensors', EDN Asia, https://www.ednasia.com/making-energy-harvesting-work-for-edge-iot-devices/, 2009. (Accessed 28 July 2022).

[20] Jacob Morgan, A Simple Explanation of 'The Internet of Things, Forbes, 2014. Accessed 28-07-2022, https://www.forbes.com/sites/jacobmorgan/2014/05/13/simple-explanation-internet-things-that-anyone-can-understand/?sh=766af2c41d09.

[21] Edith Osorio, J. Castillo, Mario Campos, Romeli Barbosa, Guillermo Becerra, Alejandro Castillo Atoche, Jaime Aguilar, 'Plant microbial fuel cells–based energy harvester system for self-powered IoT applications', Sensors 19 (2019) 1378.

[22] Takahiro Yamashita, Teppei Hayashi, Hirofumi Iwasaki, Masao Awatsu, Hiroshi Yokoyama, 'Ultra-low-power energy harvester for microbial fuel cells and its application to environmental sensing and long-range wireless data transmission', J. Power Sources 430 (2019) 1–11.

[23] K. Wetser, K. Dieleman, C. Buisman, D. Strik, 'Electricity from wetlands: tubular plant microbial fuels with silicone gas-diffusion biocathodes', Appl. Energy 185 (2017) 642–649.

[24] E. Sudirjo, P. De Jager, C.J.N. Buisman, D.P.B.T.B. Strik, Performance and long distance data acquisition via LoRa technology of a tubular plant microbial fuel cell located in a paddy field in West Kalimantan, Indonesia, Sensors (2019) 19. Switzerland.

[25] R.A. Timmers, D.P.B.T.B. Strik, H.V.M. Hamelers, C.J.N. Buisman, 'Electricity generation by a novel design tubular plant microbial fuel cell', Biomass Bioenergy 51 (2013) 60–67.

[26] M. Helder, D.P.B.T.B. Strik, H.V.M. Hamelers, R.C.P. Kuijken, C.J.N. Buisman, 'New plant-growth medium for increased power output of the Plant-Microbial Fuel Cell', Bioresour. Technol. 104 (2012) 417–423.

[27] H. Deng, Z. Chen, F. Zhao, 'Energy from plants and microorganisms: progress in plant-microbial fuel cells', ChemSusChem 5 (2012) 1006–1011.

[28] R. Regmi, R. Nitisoravut, J. Ketchaimongkol, A decade of plant-assisted microbial fuel cells: looking back and moving forward, Biofuels 9 (2018) 605–612.

[29] M. Helder, W.S. Chen, E.J.M. Van der Harst, D.P.B.T.B. Strik, H.V.M. Hamelers, C. J.N. Buisman, J. Potting, 'Electricity production with living plants on a green roof: environmental performance of the plant-microbial fuel cell', Biofuels, Bioproduct. Biorefin. 7 (2013) 52–64.

[30] N. Kaku, N. Yonezawa, Y. Kodama, K. Watanabe, 'Plant/microbe cooperation for electricity generation in a rice paddy field', Appl. Microbiol. Biotechnol. 79 (2008) 43–49.

[31] T.E. Kuleshova, N.R. Gall, A.S. Galushko, G.G. Panova, 'Electrogenesis in plant–microbial fuel cells in parallel and series connections', Tech. Phys. 66 (2021) 496–504.

[32] B. Kim, S.V. Mohan, D. Fapyane, I.S. Chang, 'Controlling voltage reversal in microbial fuel cells', Trends Biotechnol. 38 (2020) 667–678.

[33] A. Kouzuma, N. Kaku, K. Watanabe, 'Microbial electricity generation in rice paddy fields: recent advances and perspectives in rhizosphere microbial fuel cells', Appl. Microbiol. Biotechnol. 98 (2014) 9521–9526.

[34] D. Brunelli, P. Tosato, M. Rossi, Microbial fuel cell as a biosensor and a power source for flora health monitoring, in: Proceedings of IEEE Sensors, 2016.

[35] Iryna Rusyn, Oleksandr Medvediev, 'Novel Compact PMFC Based on Decorative or Culinary Plants as a Biobattery for Low-Energy Consuming Devices, Social Science Research Network (SSRN), 2023.

[36] D. Ayala-Ruiz, A. Castillo Atoche, E. Ruiz-Ibarra, E. Osorio De La Rosa, J. Vázquez Castillo, A Self-Powered PMFC-Based Wireless Sensor Node for Smart City Applications', *Wireless Communications and Mobile Computing*, 2019, 2019.

[37] HBC, Natuurgebied 'de Loozerheide'Budel-dorplein, in: Heemkundekring 'De Baronie Van Cranendonck', 2020.

[38] BV, Plant-E, 2022. https://www.plant-e.com/en/referentie-projecten/. (Accessed 9 July 2022).

[39] R.A. Timmers, D.P.B.T.B. Strik, H.V.M. Hamelers, C.J.N. Buisman, 'Characterization of the internal resistance of a plant microbial fuel cell', Electrochim. Acta 72 (2012) 165–171.

[40] A. Ter Heijne, H.V.M. Hamelers, V. De Wilde, R.A. Rozendal, C.J.N. Buisman, A bipolar membrane combined with ferric iron reduction as an efficient cathode system in microbial fuel cells, Environ. Sci. Technol. 40 (2006) 5200–5205.

[41] M. Helder, D.P.B.T.B. Strik, R.A. Timmers, S.M.T. Raes, H.V.M. Hamelers, C.J. N. Buisman, Resilience of roof-top plant-microbial fuel cells during Dutch winter, Biomass Bioenergy 51 (2013) 1–7.

[42] Engineering Toolbox, Storing Thermal Heat in Materials, 2009. https://www.engineeringtoolbox.com/sensible-heat-storage-d_1217.html.

[43] Michael T. Madigan, Kelly S. Bender, Daniel H. Buckley, W. Matthew Sattley, David Allan Stahl, Brock Biology of Microorganisms, 2018.

[44] N.H. March, M.P. Tosi, Introduction to Liquid State Physics (World Scientific). Network, the Things. 2018. "Geoffroy Gosset - LPWAN Endpoints Will Need Energy Harvesting to Achieve Scale, 2002.

[45] Raphael D. Levine, Molecular Reaction Dynamics, Cambridge University Press, Cambridge, 2005.

[46] P.M. Van Bodegom, B.K. Sorrell, A. Oosthoek, C. Bakker, R. Aerts, Separating the effects of partial submergence and soil oxygen demand on plant physiology, Ecology 89 (2008) 193–204.

[47] M.Y. Wu, E.H. Franz, S. Chen, 'Oxygen fluxes and ammonia removal efficiencies in constructed treatment wetlands', Water Environ. Res. 73 (2001) 661–666.

[48] Matsui Inoue, Tomomi, Takayoshi Tsuchiya, Interspecific differences in radial oxygen loss from the roots of three Typha species, Limnology 9 (2008) 207–211.

[49] R.A. Timmers, D.P. Strik, C. Arampatzoglou, H.V. Hamelers, C.J. Buisman, 'Radial oxygen loss decreases available substrate for electrochemically active bacteria in a PMFC', Commun. Agric. Appl. Biol. Sci. 76 (2011) 79–82.

[50] Iryna Rusyn, 'Role of microbial community and plant species in performance of plant microbial fuel cells', Renew. Sustain. Energy Rev. 152 (2021), 111697.

[51] W. Apollon, S.K. Kamaraj, H. Silos-Espino, C. Perales-Segovia, L.L. Valera-Montero, V.A. Maldonado-Ruelas, M.A. Vázquez-Gutiérrez, R.A. Ortiz-Medina, S. Flores-Benítez, J.F. Gómez-Leyva, 'Impact of Opuntia Species Plant Bio-Battery in a Semi-arid Environment: Demonstration of Their Applications, vol. 279, Applied Energy, 2020.

[52] P.G. Dennis, A.J. Miller, P.R. Hirsch, Are root exudates more important than other sources of rhizodeposits in structuring rhizosphere bacterial communities? FEMS (Fed. Eur. Microbiol. Soc.) Microbiol. Ecol. 72 (2010) 313–327.

[53] J.K. Martin, J.R. Kemp, 'Carbon loss from roots of wheat cultivars', Soil Biol. Biochem. 12 (1980) 551–554.

[54] C. Nguyen, Rhizodeposition of organic C by plants: mechanisms and controls, Agronomie 23 (2003) 375–396.

[55] P. Chong, B. Erable, A. Bergel, 'Effect of Pore Size on the Current Produced by 3-dimensional Porous Microbial Anodes: A Critical Review, Bioresource Technology, 2019, p. 289.

[56] N.S. Malvankar, M. Vargas, K.P. Nevin, A.E. Franks, C. Leang, B.C. Kim, K. Inoue, T. Mester, S.F. Covalla, J.P. Johnson, V.M. Rotello, M.T. Tuominen, D.R. Lovley, 'Tunable metallic-like conductivity in microbial nanowire networks', Nat. Nanotechnol. 6 (2011) 573–579.

[57] M.D. Yates, S.M. Strycharz-Glaven, J.P. Golden, J. Roy, S. Tsoi, J.S. Erickson, M. Y. El-Naggar, S.C. Barton, L.M. Tender, 'Measuring conductivity of living geobacter sulfurreducens biofilms', Nat. Nanotechnol. 11 (2016) 910–913.

[58] Koen Wetser, Electricity from Wetlands, Technology Assessment of the Tubular Plant Microbial Fuel Cell with an Integrated Biocathode, Wageningen University, 2016.

[59] Shaoan Cheng, Yaoli Ye, Weijun Ding, Bin Pan, Enhancing power generation of scale-up microbial fuel cells by optimizing the leading-out terminal of anode, J. Power Sources 248 (2014) 931–938.

[60] R. Rossi, P.J. Evans, B.E. Logan, 'Impact of flow recirculation and anode dimensions on performance of a large scale microbial fuel cell', J. Power Sources 412 (2019) 294–300.

[61] A. Shirpay, 'Effects of electrode size on the power generation of the microbial fuel cell by Saccharomyces cerevisiae', Ionics 27 (2021) 3967–3973.

[62] Ioannis A. Ieropoulos, John Greenman, Chris Melhuish, 'Miniature microbial fuel cells and stacks for urine utilisation', Int. J. Hydrogen Energy 38 (2013) 492–496.

[63] Eduardo D. Penteado, Carmen Maria Fernandez-Marchante, Marcelo Zaiat, Ernesto Rafael Gonzalez, Manuel Andrés Rodrigo, ' Optimization of the performance of a microbial fuel cell using the ratio electrode-surface area/anode-compartment volume', Braz. J. Chem. Eng. 35 (2018) 141–146.

[64] D.R. Bond, S.M. Strycharz-Glaven, L.M. Tender, C.I. Torres, On electron transport through geobacter biofilms, ChemSusChem 5 (2012) 1099–1105.

[65] P. Chong, B. Erable, A. Bergel, Microbial anodes: what actually occurs inside pores? Int. J. Hydrogen Energy (2019) 4484–4495.

[66] A.C.L. De Lichtervelde, A. Ter Heijne, H.V.M. Hamelers, P.M. Biesheuvel, J. E. Dykstra, Theory of ion and electron transport coupled with biochemical conversions in an electroactive biofilm, Phys. Rev. Appl. 12 (2019).

[67] K. Wetser, J. Liu, C. Buisman, D. Strik, 'Plant microbial fuel cell applied in wetlands: spatial, temporal and potential electricity generation of Spartina anglica salt marshes and Phragmites australis peat soils', Biomass Bioenergy 83 (2015) 543–550.

[68] M. Helder, D.P.B.T.B. Strik, H.V.M. Hamelers, C.J.N. Buisman, The flat-plate plant-microbial fuel cell: the effect of a new design on internal resistances, Biotechnol. Biofuels 5 (2012).

[69] I. Tou, Y.M. Azri, M. Sadi, H. Lounici, S. kebbouche-Gana, 'Chlorophytum microbial fuel cell characterization', Int. J. Green Energy 16 (2019) 947–959.

[70] Z. Ullah, S. Zeshan, 'Effect of substrate type and concentration on the performance of a double chamber microbial fuel cell', Water Sci. Technol. 81 (2020) 1336–1344.

[71] D. Wang, J. Hu, S. Hu, L. Wu, J. Xu, H. Hou, J. Yang, S. Liang, K. Xiao, B. Liu, 'Enhance cathodic capacitance to eliminate power overshoot in microbial fuel cells', J. Solid State Electrochem. 24 (2020) 1659–1667.

[72] B.E. Logan, B. Hamelers, R. Rozendal, U. Schröder, J. Keller, S. Freguia, P. Aelterman, W. Verstraete, K. Rabaey, Microbial fuel cells: methodology and technology, Environ. Sci. Technol. 40 (2006) 5181–5192.

[73] Texas Instruments, bq25570 Nano Power Boost Charger and Buck Converter for Energy Harvester Powered Applications, Texas Instruments, 2019.

[74] T.M. Linear, Ltc 3108: ultralow voltage step-up converter and power manager, in: Analog Devices Inc, 2019.